

1 State of the art of UV water treatment technologies and hydraulic design optimisation using
2 computational modelling

3 Jainil Shah^a, Audrius Židonis^b, George Aggidis^{a*}

4 a Engineering Department, Lancaster University, Lancaster, UK LA1 4YW

5 b Typhon Treatment Systems Ltd, Penrith, UK CA110BF

6 * Corresponding Author: George Aggidis - g.aggidis@lancaster.ac.uk - Engineering department,
7 Lancaster University, Lancaster, LA1 4YW, UK

8 **Keywords:** UV, Disinfection, Hydraulics, Modelling, LED,

9 **Highlights**

- 10 • Effectiveness of UV in comparison with other water disinfection technologies
- 11 • Beneficial use of CFD in optimisation of the Geometrical features of UV technology
- 12 • Investigating the effect of Geometry on the UV dose received by the water
- 13 • Exploration of various turbulence and fluence modelling affecting UV technology
- 14 • Scope and appraisal of using LED lamps in full-scale water treatment plants

15 **Abstract:**

16 Water disinfection is an essential process for drinking water use. One of the water treatment
17 process stages includes the application of Ultraviolet (UV) light to assist with the removal of
18 pathogens and viruses such as Cryptosporidium. The previous review in the UV treatment system
19 explores the optical and reaction of microorganisms to the technology. The aim of this paper is to
20 explore the hydraulics and modelling of the current technology of the UV treatment process. There
21 has been enormous progress made in the process of optimisation using Computational Fluid
22 Dynamics (CFD). Due to the expensive nature of the experiments, CFD has emerged as a vital
23 tool. This article explores two essential parts of the UV system that includes the hydraulic system
24 and the modelling. It also explores the effects of design improvements on the UV dosage and
25 overall disinfection efficiency.

26 **1.Introduction**

27 The two primary sources of potable water available for community use include surface water and
28 groundwater. Surface water contamination includes viruses, bacteria, and protozoa [1]. Thus, the
29 use of surface water for drinking purposes requires treatment through various disinfection

30 processes that involve the use of free Chlorine, Chloramine, Chlorine dioxide, Ozone and
 31 Ultraviolet Light (UV). Each of these processes is chemical processes except for the use of UV.
 32 Currently, water companies use primarily chlorinate ion for the treatment of water. However,
 33 chlorination and UV treatment have an inverse relationship in treating different types of pathogens
 34 [2]. Pathogens such as Cryptosporidium and Giardia lamblia cysts display a higher level of
 35 sensitivity to UV and are quite insensitive to the chlorination process [3]. Ozone treatment is
 36 another process that is more effective than chlorination in treating such pathogens. However, it
 37 has disadvantages, including the creation of chemicals on-site and by-products from the treatment
 38 process[1,4,5].

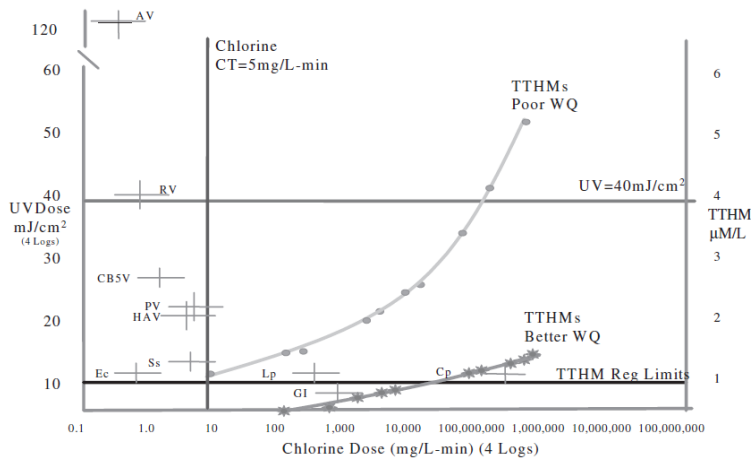
39 *Table 1: Effectiveness of disinfection processes against pathogens*

Types of pollutants	Free chlorine	Chloramine	Chlorine dioxide	Ozone	UV
Bacteria	Excellent	Good	Excellent	Excellent	Good
Viruses	Excellent	Fair	Excellent	Excellent	Fair
Protozoa	Fair to poor	poor	Good	Good	Excellent

40

41 Table 1 indicates that different pollutants possess a varying sensitivity in relation to the
 42 disinfection process [1]. Therefore, a process that includes a combination of the required
 43 properties will produce the best results for the overall water disinfection effectiveness. Using
 44 multiple disinfectants will also lead to the lower usage of chlorine, thus producing a reduced
 45 amount of chlorine by-products in the water. Figure 1 below indicates that in order to accomplish
 46 a 4-log inactivation of different pathogens, there is a varying level of dosage required in terms of
 47 UV and Chlorine. The product of intensity and irradiance time defines the UV dosage value.
 48 Combining the product of intensity and irradiance time it reduces the amount of dosage required
 49 from chlorination and UV. Increasing the UV dosage does not produce any adverse effects
 50 because there are no by-products created, although producing a higher UV dosage is expensive
 51 [2]. In addition, the combination of UV and Chlorine requires a substantially reduced amount of
 52 chlorination, which in turn produces an even smaller quantity of by-product compounds like
 53 Trihalomethanes (TTHMs). Figure 1 clearly indicates the regulatory limits for the presence of these
 54 compounds in potable water. The use of UV offers several other advantages compared to the

55 chemical processes, including the facts that it can be used instantaneously without having the
56 requirement to handle chemicals [2,4].



57

58 *Figure 1: Chlorine dose vs UV dose vs TTHM for 4 log reduction of pathogens [2]*

59

60 1.1 Current UV treatment systems

61 The current UV treatment process predominantly uses low or medium pressure mercury lamps to
62 produce UV light [6]. The medium pressure mercury lamps produce polychromatic light, i.e. light
63 in the range of 200-400 nm, while the low-pressure mercury lamps produce monochromatic light
64 and emit at 253.7nm. UV light-emitting at 260-265nm disturbs the DNA of most pathogens. Thus,
65 low-pressure lamps are more efficient compared to medium pressure mercury lamps [7]. The
66 effect of UV dosages is a measure of the effectiveness of UV treatment. The product of intensity
67 and irradiance time defines the UV dosage value [2]. The ideal system requires a uniform dosage
68 distribution inside the water reactor.

69 The classification of UV disinfection reactors includes three types of reactor, external, distributive
70 and immersive type. The external type UV reactor has the UV lamps placed outside of the water
71 flow and light transmitted through the Quartz pipe. The distributive type of reactor UV has rays
72 transmitted to the water body using a medium like a glass rod or optical fibre. The most common
73 and widely used in the industry is the immersive type of reactor. This type of reactor has lamps
74 placed inside the reactor and the flow of water around the lamps. The lamps placed perpendicular
75 or parallel to the water flow, depending on the arrangement type. Similarly, based on the UV
76 lamps' location, the classification includes two different types the contact and the non-contact
77 type. Currently, the most used contact type of reactors has mercury UV lamps inside the water

78 reactor. This is like the immersive type of water reactor [8]. Table 2 is used to summarise the type
79 of UV source used for the UV disinfection technology.

80 The validation of the UV treatment system is done using Bioassay protocol. In this test, MS2 is
81 introduced in the upstream of the flow and passed through UV reactor chamber. The sample is
82 then collected downstream of the flow. The difference in the quality of the water is analysed in
83 terms of log reduction. It requires 4 log inactivation (99.99%) of pathogens and virus for drinking
84 water application. Two different ways of measuring UV dosage is by calculating the average
85 dosage and Reduction Equivalent Dose (RED). The average dosage could give false information
86 since some pathogen might be receiving a very high dosage while some pathogens are receiving
87 low dosage. This can be overcome by calculating RED values, which calculate the minimum dose
88 received by the pathogen. Research has been done in alternative validation methods such as
89 using monitored tunable biosimetry (MTB) and using photochromic materials. However, the
90 current commercial UV treatment system is validated using biosimetry [2, 9-11].

91 *Table 2: Type of UV sources*

Type of UV source	References
Mercury - low pressure lamps	[8–31]
Mercury - medium pressure lamps	[32–37]
LED lamps	[6,7,38–59]
Source not mentioned	[2,60–72]

92 2. Modelling of UV treatment System

93 The UV modelling includes two sections: 1) modelling of the flow inside the reactor and 2)
94 Modelling of the UV fluence rate inside the reactor. The two different methodologies usually
95 adopted for modelling include SURF (Simultaneous UV fluence rate and Fluid dynamics) and
96 TURF (Three-step UV fluence rate and Fluid dynamics). The SURF method incorporates
97 simultaneous UV fluence rate and Fluid dynamics. This method defines the UV fluence rate using
98 a user-defined function in the CFD software. In comparison, the TURF method includes a three-
99 step UV fluence rate and Fluid dynamics. This method carries out separate calculations for the
100 UV fluence rate and the flow calculation [62,73]. In addition, another method used, carries out the
101 simultaneous calculation of the UV fluence rate along with the flow calculations using UDF (user-
102 defined function). However, post-processing is carried out separately using a specific written
103 code [17].

104 2.1 Modelling of flow (CFD)

105 2.1.1 Mesh

106 Mesh independency tests are carried out for the simulations. The mesh size can vary due to
107 several factors, including different sizes and other characteristics of the reactor. For some models,
108 0.5 million cells are adequate, while others require more than 2 million cells [17,62,69,73].
109 However, in these models, increasing the number of cells, the deviation of the result is less than
110 2%. Thus, the mesh considered acceptable for the result.

111 The mesh independency test carried out uses the residence time distribution of the particle paths.
112 Thus, convergence achieved at 5000 particles. Increasing the particles number does not alter the
113 residence time [22,31,74].

114 Across the flow, micro particles released at the inlet assist with understanding the flow pattern of
115 microorganisms in the water. The number of microbial particles released varies for different
116 reactors and simulations. In addition, the microbial particles size also varies. Particles assist the
117 calculation of the microbes' flow trajectories inside the reactor. The particles size is as small as
118 10^{-6} m in diameter. It is important to understand that the diameter should not affect the result of
119 the simulation [2,10,15,17,18,21,22,31,36,37,62,66,69,71,73,74].

120 2.1.2 Model settings

121 Model settings are dependent on the reactor type being a closed conduit or an open channel
122 reactor. Open channel reactors are more demanding to model as they incorporate both air and
123 water. The flow temperature considered as constant [20].

124 2.1.3 Boundary settings

125 The flow velocity and reactor conditions form the basis for the inlet and outlet conditions. Usually,
126 the inlet is applied using flow velocity perpendicular to the inlet surface. The specified inlet
127 turbulence intensity is 2% to 3%. The turbulent intensity at the inlet has little effect on the
128 simulation. The outlet conditions taken as outlet pressure, set to 0-bar gauge pressure. The walls
129 are set as no-slip boundary conditions [17,69].

130 2.1.4 Turbulence model

131 Different turbulence models such as standard k- ϵ , realisable k- ϵ , k- ω , Reynold stress model and
132 two fluid model compared for closed conduit water flow. It is worth noticing that the k- ϵ model can
133 better predict the wake-free model than the k- ω model. Thus, it predicts the upstream flow pattern
134 more accurately using k- ϵ rather than a k- ω model. However, the much more precise wake region

135 prediction uses the $k-\omega$ model. Additionally, it is also worth noting that the RSTM predicted model
136 performs better than the $k-\epsilon$ model both inside and outside the wake region. However, it is not
137 able to predict the wake region as accurately as the $k-\omega$ model. The judgement for this comparison
138 uses the experimental data from a PIV experiment. Because of the different flow pattern, there is
139 a turbulence model effect on the UV dose distribution. The difference highlighted in terms of the
140 dominant peak and secondary peak of the dose distribution. There is both dominant and
141 secondary peak in std $k-\epsilon$, realisable $k-\epsilon$, $k-\omega$, RNG and TFM. In the RTSM model, there is no
142 secondary peak, because of better flow near the wall region. $k-\omega$ has neither a dominant nor a
143 secondary peak and observes a wider spread of the UV dose distribution. The Reynold stress
144 model provides similar results for velocity and dosages but more significant variation in the
145 turbulent kinetic energy [75]. Additionally, comparison carried out for the $k-\epsilon$ model, RNG $k-\epsilon$
146 model and Reynold stress model. The $k-\epsilon$ model considered adequate, as there is a slight
147 difference in the value of velocity and dosages. The $k-\epsilon$ model is 3-4 times cheaper compared to
148 the Reynold stress model [25]. However, $k-\epsilon$ model fails to accurately predict the disinfection
149 model for certain geometry such as introduction of baffle upstream of the flow. Higher turbulence
150 model such as LES are required to correctly calculate the wakes created because of the
151 obstruction in the flow [60]. There is an effect on the mass transfer rate because of the flow in
152 certain UV processes like Advanced Oxidation Process (AOP). However, those effects are not
153 studied for the UV treatment of drinking water application [61].

154 2.2 UV modelling (UV Fluence)

155 The UV modelling helps to determine the fluence rate inside the reactor. The UV modelling carried
156 out either through user-defined function in CFD or through separate modelling using software like
157 MATLAB. There are different type of models used for modelling the fluence distribution inside the
158 reactor. Most commonly used models are MPSS and MSSS models.

159 MPSS (Multi point source summation model) model

160 The MPSS model used to simulate the fluence rate field inside the reactor. The MPSS model
161 considers each lamp as a collection of light-emitting point sources of equal power. Considers the
162 light emitted is in an axial direction. Each point receives a fluence rate equalling to the total fluence
163 rate received from each point source. The calculated light beam laws use Snell's law and Fresnel's
164 law. The calculation for the absorption law uses the Beer-Lambert's law [62,73].

165 MSSS (Multi segment source summation model)

166 The MSSS model is like the MPSS model in terms of refraction reflection and adsorption;
 167 however, it considers the lamp as a cylindrical source. The light intensity decreases with the
 168 cosine angle between the unit normal vector and the directional vector. The MSSS model is
 169 computationally expensive compared to other models [62,73]. Table 3 summarises the type of
 170 modelling software used to calculate the dosage data for the UV treatment system and the fluid
 171 data such as the turbulence model used.

172 *Table 3: Fluid flow vs Turbulence model vs UV fluence modelling*

Fluid flow modelling software	Turbulence model	UV Fluence modelling	References
Ansys Fluent	k-ε	Calc3D	[34,36]
		Integrated model in fluent	[18,19,33,64,65,69,71]
		User defined functions in fluent	[8,17,22,66]
		MATLAB	[62,73]
Ansys CFX	k-ω SST	Calc3D	[31]
COMSOL	k-ε	Not mentioned	[60,61,74]
	Large eddy simulation (LES)		[60]
	Not given		[7,41,48]
COMET	k-ε		[68]
PHOENICS			[27,29,75]
Finlab			[5]
Not required		MATLAB	[10–12,44,54,70]
Not mentioned		Not mentioned	[30,32,76,77]

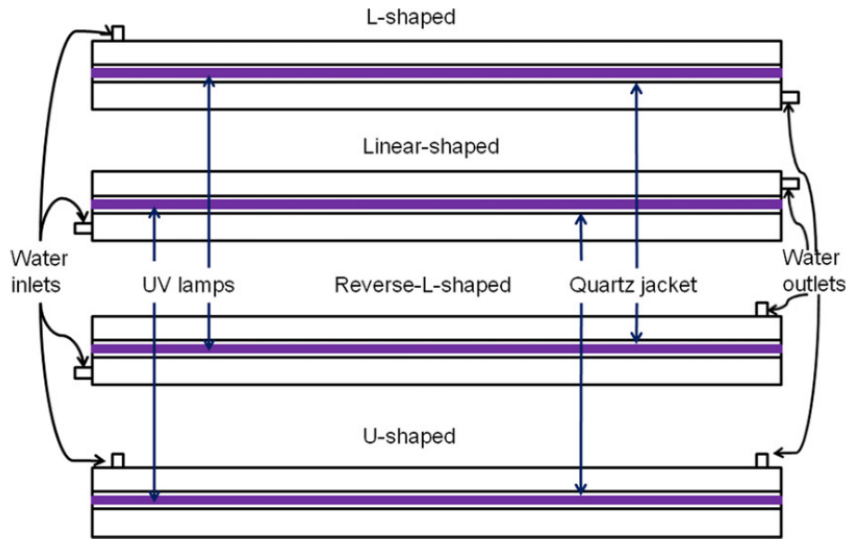
173 3. Hydraulic Systems

174 The current reactor geometry's main division includes two-sub sections, the open channel and
 175 the closed channel, reactor [37]. The closed reactors' primary use is for drinking water
 176 applications, while the open channel reactors are commonly used for wastewater applications.

177 However, there has been research carried out for open channel drinking water applications. The
178 advantages of an open channel reactor to the closed reactor include the flow that can be highly
179 turbulent, and therefore cheaper to install. Similarly, there has been research carried out for using
180 a closed reactor for wastewater applications [17,37].

181 3.1 Effect of Geometry

182 Under ideal conditions for the closed channel reactor, there is a complete mixing of the water flow
183 inside the reactor, i.e. plug flow, which will lead to equal distribution of the UV dosage. This,
184 however, is not possible in real flow conditions because the flow of particles inside the reactor is
185 unique and thus will receive unique dosage. Hence, the calculation of the UV dosage is in terms
186 of distribution rather than a fixed value [2]. There are various hydraulic features, which affect the
187 dosage received by the water. One of the easiest changes made includes the inlet and outlet
188 location. Offsetting the reactor inlet and outlet leads to better mixing of the water [25]. Based on
189 inlet-outlet location, there are different types of reactors such as L type, reverse L type, linear
190 type, and U type. The L type reactor has the inlet perpendicular to the axis of the reactor while
191 outlet is parallel. Reverse L type has an inlet parallel and outlet perpendicular to the axis of the
192 reactor. The linear type has both inlet and outlet parallel to the axis of the reactor. U type of reactor
193 has inlet and outlet both perpendicular to the axis of the reactor. U type and L type are more
194 turbulent compared to the other two because of the perpendicular inlet. L type of reactor
195 performed better than the U type of reactor for set conditions in terms of fluence distribution.
196 Geometrical changes brought different results in terms of distribution and treatment of water.
197 Changes in the dimensions of the reactor introduce changes in the dosage received by the water.
198 While in general, the increase in the length of the reactor and decreasing the cross-section area
199 of the reactor improves the reactor performance for the U type reactor. Figure 2 shows different
200 type of inlet outlet location as discussed above. [73].



201

202 *Figure 2: Layout of single lamp UV photo reactor*

203 Changes in the shape of the reactor can remove dead zones (areas that receive no dosage).
 204 Accomplished by flattening the reactor instead of the complete circular reactor. Such an
 205 improvement in the reactor can lead to reducing 37% of the lamp output for a similar dosage [74].
 206 Similarly, changes in the upstream hydraulics can also affect the dosage. 90 degree bends
 207 perpendicular and parallel to the reactor axis upstream of the reactor inlet are less efficient
 208 compared to the pipe straight to the inlet reactor [29]. Roughness of the wall produces effects not
 209 only on the hydraulics of the system but also on the dosage and RED values of the reactor. There
 210 is a drop in the velocity with an increase in the roughness value of the pipe. Compared to the
 211 smooth pipe, a rough pipe increases the value of RED depending upon the Reynolds number of
 212 the flow. At lower Reynolds numbers, there is a higher percentage difference between the smooth
 213 and the rough surface [33].

214 The above methods rely on improving the system's geometry to achieve the required amount of
 215 dosage and in addition, achieved by using reactors in series. The theoretical evaluation of
 216 reactors in the series concludes that the dosage received by two identical reactors is twice the
 217 single reactor's dosage. Hence, for treating the microorganisms, which requires two times the
 218 RED value of a single reactor, can be treated using two reactors in series [72].

219 Open channel reactors have different challenges to the closed channel reactors in terms of
 220 hydraulics of the system. As open channel reactors are mainly for wastewater applications, UVT
 221 of the water is less than 70%. UVT has an exponential relationship with UV sensitivity; hence, the
 222 treatment of highly insensitive microbes does not improve with an increase in UVT. Thus, it is

223 better to decrease the distance between the lamps to treat the microbes with higher sensitivity
224 than to increase the UVT. Like the closed channel reactor, roughness also affects the open
225 channel reactor. However, these effects are negligible for higher Reynolds numbers. Analysing
226 the open channel reactor requires a large amount of computational power. However, these
227 simulations are more cost-effective than experiments. De featuring the geometry can simplify the
228 model. A simple geometry consisting of channel and lamp provided very close results to a full-
229 scale geometry consisting of all reactors' features. The use of this can decrease the complexity
230 and cost of the simulation [17,31,37,60].

231 3.2 Effect of lamps

232 Closed channel reactors classified as parallel and perpendicular reactors, based on the
233 arrangement of the lamps. A system with lamps perpendicular to the reactor axis is classified as
234 perpendicular reactors while a system with lamps parallel to the axis of the reactor is classified
235 as parallel reactor. The effects of different configuration are complex and dependent on several
236 different other hydraulic factors. When compared to similar UV dosage and a similar number of
237 lamps, parallel lamp configuration provided better log reduction compared to the perpendicular
238 lamp configuration. These factors are highly sensitive, with small changes in location and
239 configuration results in different dosage. For example, a similar number of lamps and parallel
240 configuration, but with two different orientation types, leads to different log reduction results.
241 Lamps placed under the inlet-outlet have better log reduction compared to the evenly distributed
242 lamps inside the reactor [62,73]. The use of a genetic algorithm methodology can achieve
243 arrangement optimisation. This algorithm finds the optimum location and arrangement of lamps
244 inside the reactor for the highest minimum value of RED. The calculation for the optimum lamp
245 circle uses the following formula: $\frac{D_c}{2} \pm 20 \text{ units}$. Where D_c is the diameter of the reactor. In
246 addition, the asymmetric lamp arrangement shows better results than symmetric arrangement in
247 terms of dosage received by the microorganism. Research shows that asymmetric arrangement
248 improves RED value by 15%. The relationship between the lamp arrangement and RED is quite
249 complex, hence the use of genetic algorithm methodology to find the optimum arrangement inside
250 the reactor [34,36]. Turning off lamps one by one, can establish the importance of each lamp.
251 Turning off the lamps without removing them from the reactor to maintain similar hydraulics and
252 flow pattern inside the reactor. Using this technique, it is found that the lamps closer to the main
253 flow are more effective than the lamps away from the main flow for the overall dosage received
254 by the reactor [22].

255 A single lamp with equivalent power to six lamps performs better than six lamps. The reason for
256 this is because of the higher power and the barrier effect. Increasing the flow rate due to the
257 hydraulic pressure can minimise the barrier effect. There is the use of multi reactors in industrial
258 scale for large cross-sections. Similarly, research indicates that the single lamp reactor's energy
259 distribution is better than the double lamp reactor, while the volume emission rate is similar.
260 However, two lamps have better irradiation near the walls compared to the single lamp [71,73].

261 Using an online monitoring system can optimise the number of lamps and the configuration of the
262 lamps. Monitoring three factors, including the lamp output, attenuation coefficient, UV
263 transmission of the water and quartz sleeve-fouling coefficient. The data collected from this could
264 help in improving the efficiency of the system in real-time by changing the power of the lamps. In
265 addition, it determines the accidental breaking of lamps inside the water or cleaning required
266 inside the reactor. The increase in the lamp power increases the dosage received by the
267 microorganisms [8,13].

268 Open reactors are again subdivided into two types based on the configuration of the lamps
269 arrangement inside the open channel reactor: 1) horizontal configuration and 2) Vertical
270 configuration. The horizontal configuration is advantageous over vertical configuration in terms of
271 residence time for the microorganism. This is because the flow of water is along with the lamps
272 [17]. However, the research presents contradictory results that the vertical lamp configuration
273 performed better than the horizontal lamp configuration. In addition, staggered lamp positioning
274 is better than parallel lamp positioning in terms of RED value received by the water. The
275 differences in the value of the RED for vertical and horizontal configuration is more at lower
276 Reynolds numbers [37].

277 3.3 Effect of temperature

278 There is no temperature effect on treating the water or on the hydraulics of the system if there is
279 a continuous flow of water with small variation in the inlet temperature [22]. However, if there is a
280 significant increase in the water temperature, then relative UV intensity increases from 0.53 at
281 4.7-degree Celsius until approximately 32 degree Celsius to 1.26 after that temperature
282 decreases. This could have a significant impact if the temperature of the inlet water varies widely
283 during different seasons. The use of other factors such as varying flow rate inside the reactor can
284 offset the effect of the temperature [13]. However, it is worth noting that for three different inlet
285 temperatures of 20, 30, and 90 degrees, there is a very small change in the value of RED. Thus,
286 for the majority of the simulations, temperature effects are neglected [22].

287 3.4 Effect of UVT

288 Drinking water applications have UVT higher than 70% while wastewater application usually has
289 UVT less than 70%. Higher UVT of the water improves the dosage received by the microorganism
290 because the fluence rate inside the reactor increases exponentially with an increase in UVT.
291 Increase in UVT also leads to better energy distribution inside the reactor [8,71]. Flow rate must
292 be lower for lower UVT to allow higher residence time for the particle while, at higher UVT values,
293 the flow rate is higher [69].

294 3.5 Effect of flow rate

295 The flow rate is an essential parameter while considering the hydraulics of the reactor. Ideally, if
296 a reactor can treat all the water that flows in it, then the flow rate should be as high as possible to
297 obtain maximum efficiency out of the system. However, due to the limitations of the reactors, it is
298 not possible to attain this. Hence, it is very important to determine the ideal flow rate for each
299 system. It is not possible to carry out experiments for every change in flow rate. Hence, CFD is a
300 vital tool in determining the flow rate of the system. Current systems use different flow rates
301 ranging from as low as 1 m³/h up to as high as 552 m³/h. Low flow rates are generally used for
302 laboratory-scale experiments where the models are scaled. Industrial-scale models use higher
303 flow rates. Published research indicates the considerable amount of laboratory-scale model tests
304 carried out. However, for the industrial-scale models, such information is scarce.

305 Higher Reynolds numbers decrease the RED value, which is because there is less residence time
306 for the particle. At low Reynolds numbers, flow approaches laminar flow; this leads to too little to
307 no mixing of flow inside the reactor. At low Reynolds numbers, (usually corresponds to a low flow
308 rate) the flow is laminar. At such a low flow rate, there is little mixing of the flow. This leads to an
309 inefficient system, as the UV dosage is not uniformly distributed. At higher Reynolds numbers
310 there is proper mixing because of the swirl caused inside the reactor. This leads to a better mixing
311 of water [25]. CFD used to determine the ideal flow rate for each reactor. Each reactor because
312 of its uniqueness provides a different ideal flow rate to the system [19, 72]. Water profile plays an
313 important role, including the determination of the dosage inside the reactor. With changes in the
314 internal reactor profile, there are changes in the water profile. This, in turn, affects the path of the
315 microorganism. Due to such effect, the flow velocity is higher with lower turbulent velocity in the
316 parallel reactor compared to the vertical reactor.

317 The significant effect of hydraulics as well as the models used for the determination of the dosage
318 it has become apparent that it is essential to understand both the assumptions and the limitations

319 of the model. The method employed by researchers for the determination of the optimum flow
 320 rates for the given reactor is to initially find the optimum configuration using a constant flow rate
 321 and then using this optimum configuration to find the optimum flow rate [36]. Table 4 summarises
 322 all the effects on the UV systems.

323 *Table 4: Comparison of the type of effects on the UV systems*

Type of effects		References
Geometrical effects	Closed Channel	[22,33,34,37,69,72]
	Open channel	[13,17,31,37,68,76]
	Not mentioned	[2,13,62,72,73]
Effect of lamps		[15,22,33,34,36,37,40,42,44,49,50,56,59,61,62,67–69,71,74]
Effect of Temperature		[15,23]
Effect of UVT		[7,8,21,29,41,71]
Effect of Flow rate		[7,13,14,25,27,30,34,36,39,41,43,57,74,78–80]

324 4. Scope of UV treatment

325 DWI (water regulatory company of UK) research indicates that only 10% of current water
 326 companies use UV treatment process. Research in 2017, shows that 1492MI/d amount of water
 327 is treated using UV light from 139 units [81]. Thus, there is massive scope for the further
 328 development of the UV treatment process. As highlighted in the paper, the current system uses
 329 mercury lamps as the source of UV light for treating water at a commercial scale. Several
 330 disadvantages of mercury lamps have led to LED lamps' development as a source of UV light.
 331 The United Nations Environmental Program (UNEP) has drawn the 'Minamata Convention', which
 332 has as one of its goals the phasing out of mercury and all mercury-related products. Although this
 333 convention does not directly mention UV-Mercury lamps, it does signal the global initiative of
 334 phasing out the usage of mercury [82]. Table 5 summarises the advantages and disadvantages
 335 of the mercury system against the LED system. Wide range of research has proven LED at bench
 336 scale to be effective in disinfecting water [6]. Recently there is advancement in terms of
 337 developing the first full-scale UV-LED drinking water disinfection. This full-scale LED-UV

338 treatment plant is being used for municipal water treatment work and is equivalent to the mercury-
339 based UV treatment in terms of water quality [52].

340 *Table 5: Comparison of Mercury lamps vs LED lamps*

	Mercury Lamps	LED lamps
Material	Usage of very toxic material	No issues as such in LED lamps
Response time	It takes time to heat up mercury lamps	They operate quicker and do not have any lead time
Energy efficient	Less efficient	More efficient
Life span	Shorter life span	Long life span
Carbon footprint	Bigger carbon footprint	Comparatively smaller footprint

341

342 5. Conclusions

343 Mercury lamps have been dominating technology in UV treatment process so far. The CFD
344 models are pivotal and decisive in the development of the UV technology. The CFD models can
345 predict the dosage received by the water considerably better than just applying the average
346 dosage to the system based on the power of lamps. Using CFD models and the fluence model
347 benefits the flow prediction and unlocks the opportunity to optimise the model for its most efficient
348 application. The limitations and the disadvantages of the current commercial system has paved
349 way for the research in the LED lamps as a source for the generation of UV light. More research
350 is required for the development of LED lamps capable of handling a large quantity of water.

351 Acknowledgements

352 This work is funded by Lancaster University through European Regional Development
353 Fund, Centre of Global Eco-Innovation, and industrial partners Typhon Treatment Systems Ltd.

354 References

355

- 356 [1] G. Howe, Kerry J. Hand, David W. Crittenden, John C. Trussell, R. Rhodes
357 Tchobanoglous, Disinfection, in: *Princ. Water Treat.*, 3rd ed., John Wiley & Sons, 2012:
358 pp. 525–583.
- 359 [2] Y.A. Lawryshyn, B. Cairns, UV disinfection of water: The need for UV reactor validation,
360 *Water Sci. Technol. Water Supply*. 3 (2003) 293–300.
361 <https://doi.org/10.2166/ws.2003.0075>.
- 362 [3] K.G. LINDEN, G. Faubert, W. Cairns, M.D. Sobsey, UV Disinfection of *Giardia lamblia*
363 Cysts in Water, *Environ. Sci. Technol.* 36 (2002) 2519–2522.
- 364 [4] J. Zhang, A.E. Tejada-Martínez, Q. Zhang, Developments in computational fluid
365 dynamics-based modeling for disinfection technologies over the last two decades: A
366 review, *Environ. Model. Softw.* 58 (2014) 71–85.
367 <https://doi.org/10.1016/j.envsoft.2014.04.003>.
- 368 [5] B.A. Wols, J.A.M.H. Hofman, W.S.J. Uijtewaal, L.C. Rietveld, J.C. van Dijk, Evaluation of
369 different disinfection calculation methods using CFD, *Environ. Model. Softw.* 25 (2010)
370 573–582. <https://doi.org/10.1016/j.envsoft.2009.09.007>.
- 371 [6] K. Song, M. Mohseni, F. Taghipour, Application of ultraviolet light-emitting diodes (UV-
372 LEDs) for water disinfection: A review, *Water Res.* 94 (2016) 341–349.
373 <https://doi.org/10.1016/j.watres.2016.03.003>.
- 374 [7] R.M. Jenny, M.N. Jasper, O.D. Simmons, M. Shatalov, J.J. Ducoste, Heuristic
375 optimization of a continuous flow point-of-use UV-LED disinfection reactor using
376 computational fluid dynamics, *Water Res.* 83 (2015) 310–318.
377 <https://doi.org/10.1016/j.watres.2015.06.031>.
- 378 [8] H.Y. Li, H. Osman, C.W. Kang, T. Ba, Numerical and experimental investigation of UV
379 disinfection for water treatment, *Appl. Therm. Eng.* 111 (2017) 280–291.
380 <https://doi.org/10.1016/j.applthermaleng.2016.09.106>.
- 381 [9] M. Li, Z. Qiang, C. Wang, J.R. Bolton, J. Lian, Development of monitored tunable
382 biosimetry for fluence validation in an ultraviolet disinfection reactor, *Sep. Purif.*
383 *Technol.* 117 (2013) 12–17. <https://doi.org/10.1016/j.seppur.2013.01.021>.
- 384 [10] M. Brahmi, A. Hassen, Disinfection of Wastewater by UV Irradiation: Influence of
385 Hydrodynamics on the Performance of the Disinfection, *Environ. Eng. Res.* 16 (2011)
386 243–252. <https://doi.org/10.4491/eer.2011.16.4.243>.
- 387 [11] G. Imoberdorf, M. Mohseni, Modeling and experimental evaluation of vacuum-UV
388 photoreactors for water treatment, *Chem. Eng. Sci.* 66 (2011) 1159–1167.
389 <https://doi.org/10.1016/j.ces.2010.12.020>.
- 390 [12] V.N. Gandhi, P.J.W. Roberts, J.H. Kim, Visualizing and quantifying dose distribution in a
391 UV reactor using three-dimensional laser-induced fluorescence, *Environ. Sci. Technol.* 46
392 (2012) 13220–13226. <https://doi.org/10.1021/es303133f>.
- 393 [13] Z. Qiang, M. Li, J.R. Bolton, Development of a tri-parameter online monitoring system for
394 UV disinfection reactors, *Chem. Eng. J.* 222 (2013) 101–107.
395 <https://doi.org/10.1016/j.cej.2013.02.046>.

- 396 [14] Z. Qiang, M. Li, J.R. Bolton, J. Qu, C. Wang, Estimating the fluence delivery in UV
397 disinfection reactors using a “detector-model” combination method, *Chem. Eng. J.* 233
398 (2013) 39–46. <https://doi.org/10.1016/j.cej.2013.08.024>.
- 399 [15] M. Li, Z. Qiang, J.R. Bolton, In situ detailed fluence rate distributions in a UV reactor with
400 multiple low-pressure lamps: Comparison of experimental and model results, *Chem. Eng.*
401 *J.* 214 (2013) 55–62. <https://doi.org/10.1016/j.cej.2012.10.024>.
- 402 [16] M. Bagheri, M. Mohseni, Computational fluid dynamics (CFD) modeling of VUV/UV
403 photoreactors for water treatment, *Chem. Eng. J.* 256 (2014) 51–60.
404 <https://doi.org/10.1016/j.cej.2014.06.068>.
- 405 [17] R.K. Saha, M. Ray, C. Zhang, Computational fluid dynamics simulation and parametric
406 study of an open channel ultra-violet wastewater disinfection reactor, *Water Qual. Res. J.*
407 *Canada.* 50 (2015) 58–71. <https://doi.org/10.2166/wqrjc.2014.034>.
- 408 [18] W. Li, M. Li, J.R. Bolton, Z. Qiang, Configuration optimization of UV reactors for water
409 disinfection with computational fluid dynamics: Feasibility of using particle minimum UV
410 dose as a performance indicator, *Chem. Eng. J.* 306 (2016) 1–8.
411 <https://doi.org/10.1016/j.cej.2016.07.042>.
- 412 [19] W. Li, M. Li, J.R. Bolton, J. Qu, Z. Qiang, Impact of inner-wall reflection on UV reactor
413 performance as evaluated by using computational fluid dynamics: The role of diffuse
414 reflection, *Water Res.* 109 (2017) 382–388. <https://doi.org/10.1016/j.watres.2016.11.068>.
- 415 [20] M.L. Janex, P. Savoye, Z. Do-Quang, E. Blatchley, J.M. Laîné, Impact of water quality
416 and reactor hydrodynamics on wastewater disinfection by UV, use of CFD modeling for
417 performance optimization, *Water Sci. Technol.* 38 (1998) 71–77.
418 [https://doi.org/10.1016/S0273-1223\(98\)00567-8](https://doi.org/10.1016/S0273-1223(98)00567-8).
- 419 [21] A.W. Schmalwieser, G. Hirschmann, A. Cabaj, R. Sommer, Method to determine the
420 power efficiency of UV disinfection plants and its application to low pressure plants for
421 drinking water, *Water Sci. Technol. Water Supply.* 17 (2017) 947–957.
422 <https://doi.org/10.2166/ws.2016.185>.
- 423 [22] H. Sobhani, H. Shokouhmand, Effects of number of low-pressure ultraviolet lamps on
424 disinfection performance of a water reactor, *J. Water Process Eng.* 20 (2017) 97–105.
425 <https://doi.org/10.1016/j.jwpe.2017.08.021>.
- 426 [23] J. Xing, H. Wang, X. Cheng, X. Tang, X. Luo, J. Wang, T. Wang, G. Li, H. Liang,
427 Application of low-dosage UV/chlorine pre-oxidation for mitigating ultrafiltration (UF)
428 membrane fouling in natural surface water treatment, *Chem. Eng. J.* 344 (2018) 62–70.
429 <https://doi.org/10.1016/j.cej.2018.03.052>.
- 430 [24] D.B. Miklos, C. Remy, M. Jekel, K.G. Linden, J.E. Drewes, U. Hübner, Evaluation of
431 advanced oxidation processes for water and wastewater treatment – A critical review,
432 *Water Res.* 139 (2018) 118–131. <https://doi.org/10.1016/j.watres.2018.03.042>.
- 433 [25] N.G. Wright, D.M. Hargreaves, The use of CFD in the evaluation of UV treatment
434 systems, *J. Hydroinformatics.* 3 (2001) 59–70.
435 <http://www.iwaponline.com/jh/003/jh0030059.htm>.
- 436 [26] F. Solari, G. Girolimetti, R. Montanari, G. Vignali, A New Method for the Validation of
437 Ultraviolet Reactors by Means of Photochromic Materials, *Food Bioprocess Technol.* 8
438 (2015) 2192–2211. <https://doi.org/10.1007/s11947-015-1581-1>.

- 439 [27] J. Ducoste, D. Liu, K. Linden, Alternative approaches to modeling fluence distribution and
440 microbial inactivation in ultraviolet reactors: Lagrangian versus Eulerian, *J. Environ. Eng.*
441 (2005) 1393–1403. [https://doi.org/10.1061/\(ASCE\)0733-9372\(2005\)131:10\(1393\)](https://doi.org/10.1061/(ASCE)0733-9372(2005)131:10(1393)).
- 442 [28] H. Mamane, Impact of particles on UV disinfection of water and wastewater effluents: A
443 review, *Rev. Chem. Eng.* 24 (2008) 67–157. [https://doi.org/10.1515/REVCE.2008.24.2-](https://doi.org/10.1515/REVCE.2008.24.2-3.67)
444 3.67.
- 445 [29] X. Zhao, S.M. Alpert, J.J. Ducoste, Assessing the impact of upstream hydraulics on the
446 dose distribution of ultraviolet reactors using fluorescence microspheres and
447 computational fluid dynamics, *Environ. Eng. Sci.* 26 (2009) 947–959.
448 <https://doi.org/10.1089/ees.2008.0139>.
- 449 [30] E. Siamak, T. Fariborz, Simulation of UV photoreactor for degradation of chemical
450 contaminants: Model development and evaluation, *Environ. Sci. Technol.* 44 (2010)
451 2056–2063. <https://doi.org/10.1021/es902391t>.
- 452 [31] J.G. Bak, W. Hwang, J. Cho, Geometry defeaturing effects in CFD model-based
453 assessment of an open-channel-type UV wastewater disinfection system, *Water*
454 (Switzerland). 9 (2017). <https://doi.org/10.3390/w9090641>.
- 455 [32] H. Pan, M. Orava, Performance evaluation of the UV disinfection reactors by CFD and
456 fluence simulations using a concept of disinfection efficiency, *J. Water Supply Res.*
457 *Technol. - AQUA.* 56 (2007) 181–189. <https://doi.org/10.2166/aqua.2007.101>.
- 458 [33] T. Sultan, S. Ahmad, J. Cho, Numerical study of the effects of surface roughness on
459 water disinfection UV reactor, *Chemosphere.* 148 (2016) 108–117.
460 <https://doi.org/10.1016/j.chemosphere.2016.01.005>.
- 461 [34] T. Sultan, Z. Ahmad, Z. Anwar, M. Shahzad Khurram, Impact of asymmetric lamp
462 positioning on the performance of a closed-conduit UV reactor, *Ain Shams Eng. J.* 8
463 (2017) 225–235. <https://doi.org/10.1016/j.asej.2016.08.022>.
- 464 [35] S.E. Beck, H.B. Wright, T.M. Hargy, T.C. Larason, K.G. Linden, Action spectra for
465 validation of pathogen disinfection in medium-pressure ultraviolet (UV) systems, *Water*
466 *Res.* 70 (2015) 27–37. <https://doi.org/10.1016/j.watres.2014.11.028>.
- 467 [36] T. Sultan, Z. Ahmad, J. Cho, Optimization of lamp arrangement in a closed-conduit UV
468 reactor based on a genetic algorithm, *Water Sci. Technol.* 73 (2016) 2526–2543.
469 <https://doi.org/10.2166/wst.2016.119>.
- 470 [37] T. Sultan, Numerical study of the effects of lamp configuration and reactor wall roughness
471 in an open channel water disinfection UV reactor, *Chemosphere.* 155 (2016) 170–179.
472 <https://doi.org/10.1016/j.chemosphere.2016.04.050>.
- 473 [38] A. Gross, F. Stangl, K. Hoenes, M. Sift, M. Hessling, Improved drinking water disinfection
474 with UVC-LEDs for *Escherichia coli* and *Bacillus subtilis* utilizing quartz tubes as light
475 guide, *Water* (Switzerland). 7 (2015) 4605–4621. <https://doi.org/10.3390/w7094605>.
- 476 [39] M.A. Würtele, T. Kolbe, M. Lipsz, A. Külberg, M. Weyers, M. Kneissl, M. Jekel,
477 Application of GaN-based ultraviolet-C light emitting diodes - UV LEDs - for water
478 disinfection, *Water Res.* 45 (2011) 1481–1489.
479 <https://doi.org/10.1016/j.watres.2010.11.015>.
- 480 [40] A.C. Chevremont, A.M. Farnet, B. Coulomb, J.L. Boudenne, Effect of coupled UV-A and
481 UV-C LEDs on both microbiological and chemical pollution of urban wastewaters, *Sci.*

- 482 Total Environ. 426 (2012) 304–310. <https://doi.org/10.1016/j.scitotenv.2012.03.043>.
- 483 [41] R.M. Jenny, O.D. Simmons, M. Shatalov, J.J. Ducoste, Modeling a continuous flow
484 ultraviolet Light Emitting Diode reactor using computational fluid dynamics, Chem. Eng.
485 Sci. 116 (2014) 524–535. <https://doi.org/10.1016/j.ces.2014.05.020>.
- 486 [42] M.P. Akgün, S. Ünlütürk, Effects of ultraviolet light emitting diodes (LEDs) on microbial
487 and enzyme inactivation of apple juice, Int. J. Food Microbiol. 260 (2017) 65–74.
488 <https://doi.org/10.1016/j.ijfoodmicro.2017.08.007>.
- 489 [43] G.Y. Lui, D. Roser, R. Corkish, N. Ashbolt, P. Jagals, R. Stuetz, Photovoltaic powered
490 ultraviolet and visible light-emitting diodes for sustainable point-of-use disinfection of
491 drinking waters, Sci. Total Environ. 493 (2014) 185–196.
492 <https://doi.org/10.1016/j.scitotenv.2014.05.104>.
- 493 [44] A. Kheyrandish, M. Mohseni, F. Taghipour, Development of a method for the
494 characterization and operation of UV-LED for water treatment, Water Res. 122 (2017)
495 570–579. <https://doi.org/10.1016/j.watres.2017.06.015>.
- 496 [45] S. Rattanukul, K. Oguma, Inactivation kinetics and efficiencies of UV-LEDs against
497 *Pseudomonas aeruginosa*, *Legionella pneumophila*, and surrogate microorganisms,
498 Water Res. 130 (2018) 31–37. <https://doi.org/10.1016/j.watres.2017.11.047>.
- 499 [46] N.M. Hull, K.G. Linden, Synergy of MS2 disinfection by sequential exposure to tailored
500 UV wavelengths, Water Res. 143 (2018) 292–300.
501 <https://doi.org/10.1016/j.watres.2018.06.017>.
- 502 [47] Y. Qiao, D. Chen, D. Wen, Use of coupled wavelength ultraviolet light-emitting diodes for
503 inactivation of bacteria in subsea oil-field injection water, Sci. Total Environ. 640–641
504 (2018) 757–763. <https://doi.org/10.1016/j.scitotenv.2018.05.283>.
- 505 [48] C. Bowker, A. Sain, M. Shatalov, J. Ducoste, Microbial UV fluence-response assessment
506 using a novel UV-LED collimated beam system, Water Res. 45 (2011) 2011–2019.
507 <https://doi.org/10.1016/j.watres.2010.12.005>.
- 508 [49] P.O. Nyangaresi, Y. Qin, G. Chen, B. Zhang, Y. Lu, L. Shen, Effects of single and
509 combined UV-LEDs on inactivation and subsequent reactivation of *E. coli* in water
510 disinfection, Water Res. 147 (2018) 331–341.
511 <https://doi.org/10.1016/j.watres.2018.10.014>.
- 512 [50] Y. Xiao, X.N. Chu, M. He, X.C. Liu, J.Y. Hu, Impact of UVA pre-radiation on UVC
513 disinfection performance: Inactivation, repair and mechanism study, Water Res. 141
514 (2018) 279–288. <https://doi.org/10.1016/j.watres.2018.05.021>.
- 515 [51] X.Y. Zou, Y.L. Lin, B. Xu, T.C. Cao, Y.L. Tang, Y. Pan, Z.C. Gao, N.Y. Gao, Enhanced
516 inactivation of *E. coli* by pulsed UV-LED irradiation during water disinfection, Sci. Total
517 Environ. 650 (2019) 210–215. <https://doi.org/10.1016/j.scitotenv.2018.08.367>.
- 518 [52] P. Jarvis, O. Autin, E.H. Goslan, F. Hassard, Application of ultraviolet light-emitting
519 diodes (UV-LED) to full-scale drinking-water disinfection, Water (Switzerland). 11 (2019).
520 <https://doi.org/10.3390/w11091894>.
- 521 [53] G.Q. Li, Z.Y. Huo, Q.Y. Wu, Y. Lu, H.Y. Hu, Synergistic effect of combined UV-LED and
522 chlorine treatment on *Bacillus subtilis* spore inactivation, Sci. Total Environ. 639 (2018)
523 1233–1240. <https://doi.org/10.1016/j.scitotenv.2018.05.240>.

- 524 [54] A. Kheyrandish, F. Taghipour, M. Mohseni, UV-LED radiation modeling and its
525 applications in UV dose determination for water treatment, *J. Photochem. Photobiol. A*
526 *Chem.* 352 (2018) 113–121. <https://doi.org/10.1016/j.jphotochem.2017.10.047>.
- 527 [55] S.E. Beck, H. Ryu, L.A. Boczek, J.L. Cashdollar, K.M. Jeanis, J.S. Rosenblum, O.R.
528 Lawal, K.G. Linden, Evaluating UV-C LED disinfection performance and investigating
529 potential dual-wavelength synergy, *Water Res.* 109 (2017) 207–216.
530 <https://doi.org/10.1016/j.watres.2016.11.024>.
- 531 [56] K. Song, F. Taghipour, M. Mohseni, Microorganisms inactivation by continuous and
532 pulsed irradiation of ultraviolet light-emitting diodes (UV-LEDs), *Chem. Eng. J.* 343 (2018)
533 362–370. <https://doi.org/10.1016/j.cej.2018.03.020>.
- 534 [57] W.-L. Wang, Q.-Y. Wu, Z.-M. Li, Y. Lu, Y. Du, T. Wang, N. Huang, H.-Y. Hu, Light-
535 emitting diodes as an emerging UV source for UV/chlorine oxidation: Carbamazepine
536 degradation and toxicity changes, *Chem. Eng. J.* 310 (2017) 148–156.
537 <https://doi.org/10.1016/j.cej.2016.10.097>.
- 538 [58] K. Oguma, R. Kita, H. Sakai, M. Murakami, S. Takizawa, Application of UV light emitting
539 diodes to batch and flow-through water disinfection systems, *Desalination.* 328 (2013)
540 24–30. <https://doi.org/10.1016/j.desal.2013.08.014>.
- 541 [59] G.Q. Li, W.L. Wang, Z.Y. Huo, Y. Lu, H.Y. Hu, Comparison of UV-LED and low pressure
542 UV for water disinfection: Photoreactivation and dark repair of *Escherichia coli*, *Water*
543 *Res.* 126 (2017) 134–143. <https://doi.org/10.1016/j.watres.2017.09.030>.
- 544 [60] B.A. Wols, W.S.J. Uijtewaald, J.A.M.H. Hofman, L.C. Rietveld, J.C. van Dijk, The
545 weaknesses of a k- ϵ model compared to a large-eddy simulation for the prediction
546 of UV dose distributions and disinfection, *Chem. Eng. J.* 162 (2010) 528–536.
547 <https://doi.org/10.1016/j.cej.2010.05.055>.
- 548 [61] B.A. Wols, D.J.H. Harmsen, T. van Remmen, E.F. Beerendonk, C.H.M. Hofman-Caris,
549 Design aspects of UV/H₂O₂ reactors, *Chem. Eng. Sci.* 137 (2015) 712–721.
550 <https://doi.org/10.1016/j.ces.2015.06.061>.
- 551 [62] C. Xu, G.P. Rangaiah, X.S. Zhao, A computational study of the effect of lamp
552 arrangements on the performance of ultraviolet water disinfection reactors, *Chem. Eng.*
553 *Sci.* 122 (2015) 299–306. <https://doi.org/10.1016/j.ces.2014.09.041>.
- 554 [63] C. Powell, Y. Lawryshyn, Standard Methodology for Transient Simulations of UV
555 Disinfection Reactors, 2017. [https://doi.org/10.1061/\(ASCE\)EE.1943-7870.0001153](https://doi.org/10.1061/(ASCE)EE.1943-7870.0001153).
- 556 [64] W. Li, M. Li, D. Wen, Z. Qiang, Development of economical-running strategy for multi-
557 lamp UV disinfection reactors in secondary water supply systems with computational fluid
558 dynamics simulations, *Chem. Eng. J.* 343 (2018) 317–323.
559 <https://doi.org/10.1016/j.cej.2018.03.017>.
- 560 [65] D.A. Sozzi, F. Taghipour, UV reactor performance modeling by Eulerian and Lagrangian
561 methods, *Environ. Sci. Technol.* 40 (2006) 1609–1615.
562 <https://doi.org/10.1021/es051006x>.
- 563 [66] A. Sozzi, F. Taghipour, The importance of hydrodynamics in UV advanced oxidation
564 reactors, *Water Sci. Technol.* 55 (2007) 53–58. <https://doi.org/10.2166/wst.2007.378>.
- 565 [67] C. Li, B. Deng, C.N. Kim, A numerical prediction on the reduction of microorganisms with
566 UV disinfection, *J. Mech. Sci. Technol.* 24 (2010) 1465–1473.

- 567 <https://doi.org/10.1007/s12206-010-0502-5>.
- 568 [68] B.A. Younis, T.H. Yang, Computational modeling of ultraviolet disinfection, *Water Sci.*
569 *Technol.* 62 (2010) 1872–1878. <https://doi.org/10.2166/wst.2010.469>.
- 570 [69] J. Chen, B. Deng, C.N. Kim, Computational fluid dynamics (CFD) modeling of UV
571 disinfection in a closed-conduit reactor, *Chem. Eng. Sci.* 66 (2011) 4983–4990.
572 <https://doi.org/10.1016/j.ces.2011.06.043>.
- 573 [70] T. Coenen, W. Van de Moortel, F. Logist, J. Luyten, J.F.M. Van Impe, J. Degève,
574 Modeling and geometry optimization of photochemical reactors: Single- and multi-lamp
575 reactors for UV-H₂O₂AOP systems, *Chem. Eng. Sci.* 96 (2013) 174–189.
576 <https://doi.org/10.1016/j.ces.2013.03.056>.
- 577 [71] G. Asadollahfardi, M. Molaei, M. Taheriyoun, I. Leversage, Comparison of ultraviolet (UV)
578 radiation intensity between a single lamp and a double lamp in a reactors, *Water Pract.*
579 *Technol.* 9 (2014) 558–565. <https://doi.org/10.2166/wpt.2014.062>.
- 580 [72] Y. Lawryshyn, R. Hofmann, Theoretical Evaluation of UV Reactors in Series, *J. Environ.*
581 *Eng.* 141 (2015) 04015023. [https://doi.org/10.1061/\(ASCE\)EE.1943-7870.0000924](https://doi.org/10.1061/(ASCE)EE.1943-7870.0000924).
- 582 [73] C. Xu, X.S. Zhao, G.P. Rangaiah, Performance analysis of ultraviolet water disinfection
583 reactors using computational fluid dynamics simulation, *Chem. Eng. J.* 221 (2013) 398–
584 406. <https://doi.org/10.1016/j.ces.2013.01.108>.
- 585 [74] B.A. Wols, L. Shao, W.S.J. Uijttewaai, J.A.M.H. Hofman, L.C. Rietveld, J.C. van Dijk,
586 Evaluation of experimental techniques to validate numerical computations of the
587 hydraulics inside a UV bench-scale reactor, *Chem. Eng. Sci.* 65 (2010) 4491–4502.
588 <https://doi.org/10.1016/j.ces.2010.04.013>.
- 589 [75] D. Liu, C. Wu, K. Linden, J. Ducoste, Numerical simulation of UV disinfection reactors:
590 Evaluation of alternative turbulence models, *Appl. Math. Model.* 31 (2007) 1753–1769.
591 <https://doi.org/10.1016/j.apm.2006.06.004>.
- 592 [76] K. Chiu, D.A. Lyn, P. Savoye, E.R. Blatchley III, Integrated UV Disinfection Model Based
593 on Particle Tracking, *J. Environ. Eng.* 125 (1999) 7–16.
594 [https://doi.org/10.1061/\(ASCE\)0733-9372\(1999\)125:1\(7\)](https://doi.org/10.1061/(ASCE)0733-9372(1999)125:1(7)).
- 595 [77] B.A. Younis, T.H. Yang, Prediction of the effects of vortex shedding on UV disinfection
596 efficiency, *J. Water Supply Res. Technol. - AQUA.* 60 (2011) 147–158.
597 <https://doi.org/10.2166/aqua.2011.008>.
- 598 [78] C.J. Noakes, P.A. Sleight, L.A. Fletcher, C.B. Beggs, Use of CFD modelling to optimise
599 the design of upper-room UVGI disinfection systems for ventilated rooms, *Indoor Built*
600 *Environ.* 15 (2006) 347–356. <https://doi.org/10.1177/1420326X06067353>.
- 601 [79] G. He, T. Zhang, F. Zheng, Q. Zhang, An efficient multi-objective optimization method for
602 water quality sensor placement within water distribution systems considering
603 contamination probability variations, *Water Res.* 143 (2018) 165–175.
604 <https://doi.org/10.1016/j.watres.2018.06.041>.
- 605 [80] H. Zhou, D.W. Smith, Advanced technologies in water and wastewater treatment, *Can. J.*
606 *Civ. Eng.* 28 (2001) 49–66. <https://doi.org/10.1139/l00-091>.
- 607 [81] D.S. Glenn Dillon, Tom Hall, Comparison of Private Water Supply and Public Water
608 Supply Ultraviolet(UV) Systems: Final Report, 2016.

609 <http://www.dwi.gov.uk/research/completed-research/reports/DWI70-2-306.pdf>.

610 [82] Minamata convention on mercury, United Nations. (2019) 72.

611 <http://www.mercuryconvention.org/Portals/11/documents/Booklets/COP3->

612 [version/Minamata-Convention-booklet-Sep2019-EN.pdf](http://www.mercuryconvention.org/Portals/11/documents/Booklets/COP3-version/Minamata-Convention-booklet-Sep2019-EN.pdf) (accessed September 13, 2020).

613